Long-range hydrodynamic forces in liquid FM-AFM

Clémence Devailly, Patrick Bouriat, Christophe Dicharry, Frédéric Risso, Thierry Ondarçuhu, Philippe Tordjeman

Long-range hydrodynamic forces in liquid FM-AFM

Clémence Devailly[1], Patrick Bouriat[2], Christophe Dicharry[2], Frédéric Risso[1], Thierry Ondarçuhu[1] and Philippe Tordjeman[1]

[1] Institut de Mécanique des Fluides de Toulouse (IMFT), Université de Toulouse, CNRS, Toulouse, France
[2] Université de Pau et des Pays de l'Adour, E2S UPPA, CNRS, TOTAL, UMR5150, Laboratoire des fluides complexes et leurs réservoirs, Pau, France.

E-mail: philippe.tordjeman@imft.fr

Abstract

We study the effects of hydrodynamic forces in frequency-modulation AFM experiments (FM-AFM) in liquid. We first establish the theoretical equations needed to derive the interaction stiffness k_{int} and the damping β_{int} due to the hydrodynamic forces from the frequency shift and the excitation amplitude. We develop specific FM-AFM experiments to measure the variation of k_{int} and β_{int} over a large range of distance in water up to 200 μm. Comparison between theory and experiments point out that the evolution of k_{int} at short and long distance arises from unsteady hydrodynamic forces on the cantilever. On the other hand, β_{int} is small at long distance and diverges at short probe-surface distance, as predicted by the classical Reynolds sphere model.

Supplementary material for this article is available online

Keywords: atomic force microscopy, hydrodynamic force, frequency modulation

(Some figures may appear in colour only in the online journal)

1. Introduction

Nanoscale imaging and investigation of local properties of materials by atomic force microscopy (AFM) requires a comprehensive understanding of the interaction forces between the probe and the material under study. In general, these interaction forces may have conservative and dissipative components [1] leading to in-phase and out-of-phase responses compared to the excitation signal, respectively. The dynamic AFM techniques based on the cantilever oscillation, allow to quantify both contributions. In Amplitude Modulation (AM-AFM), the variations of the amplitude and of the phase, when the probe approaches the material surface, depend on both the conservative and dissipative forces [2]. In Frequency Modulation (FM-AFM), in air or vacuum, the in-phase and out-of-phase contributions are obtained independently by monitoring the resonance frequency and the excitation voltage to maintain the tip oscillation amplitude constant, respectively [3]. This constitutes an advantage of FM-AFM compared to AM-AFM.

Performing AFM in liquids is of a great interest, in particular with biological samples which need to remain immersed [4] or to study molecules or ion adsorption at solid interfaces [5, 6]. Contact mode and dynamic AFM mode have been intensively used leading to high-resolution imaging of biological samples and high speed monitoring of biological processes [7]. However, dynamic AFM in liquids is a lot more tricky than in air due to the dynamic viscosity of the medium η which is, for water, 50 higher than in air [8]. Dissipative hydrodynamic forces become significant and lead to a dramatic decrease of the quality factor of the cantilever (from 100 in air to unit in water) and, consequently of the sensitivity. Moreover, cantilever base motion in dynamic mode becomes significant compared to the cantilever end amplitude. Additional vibration of the cantilever can also be induced by the liquid cell or the cantilever holder [9, 10]. In order to perform FM-AFM measurements in liquids these effects have to be taken into account in the general equations as it was done in AM-AFM [10, 11]. The theoretical equations that allow to calculate the

hydrodynamic load of a microcantilever that vibrates in a viscous fluid close to a surface were solved numerically [12–14]. These results established that the in-phase and out-of-phase components of the hydrodynamic force strongly depend on the Reynolds number $\mathrm{Re} = \rho\omega b^2/4\eta$, where ρ, ω and b are the fluid density, the oscillation angular frequency and the width of the cantilever, respectively. Moreover, the two components may be of the same order of magnitude due to a sizable increase of the added-mass coefficient when the surface-cantilever distance decreases [14]. FM-AFM experiments performed with cantilevers functionalized by a bead or with large radius tips show that the dissipative force is well described by the Reynolds force [11, 15–17] (low Re). However, the in-phase part of the force may change as well, even in simple liquids where no elastic part is expected. This change has been several times seen in literature as a phase decrease in AM mode [11] or as a frequency shift in FM mode [16]. In these experiments, the frequency shift varies spatially in a micron range, much larger than the characteristic length of molecular interactions. An example of the frequency shift variation when a 8 μ m glass bead is approached to a silica surface in water is presented figure 1 (see below for details). This long-range variation shows that hydrodynamic forces play a significant role in dynamic AFM.

In order to decorrelate the hydrodynamic force and the interaction force in FM-AFM, the first one should be calculated in function of the tip-sample distance and subtracted to the measured total force. Even if the theoretical equations are well described in the literature, the calculation of the hydrodynamic load requires numerical simulations which are difficult to apply in practice. Furthermore, to our knowledge, direct comparison between experiments and theory has never been achieved because no experiments in FM-AFM were realized at very large distance.

In this paper, we propose an alternative solution for FM-AFM experiments in liquid: we first derive the general relations for the frequency shift and the excitation tension for FM-AFM experiments in liquids. As expected, we show that these two signals are not anymore independently related to the conservative and dissipative forces as in air. Then, we develop specific experiments at very large distance to measure the in-phase and the out-of-phase components of the hydrodynamic load in function of the cantilever-surface distance. The results can be reproduced by a pure hydrodynamic model, in a simple geometry, which provides an analytical derivation of the two components, and remains valid even at short distance where the dissipation is modeled by the Reynolds equation.

2. FM-AFM theory in liquids

We derive the general equations to extract physical quantities FM-AFM in liquids when the resonance quality factor Q is small. We consider that the cantilever is fixed on a base, excited at an amplitude $\mathbf{A}$ which has about the same magnitude as the tip deflection $\mathbf{q}$. The model for a cantilever excited by a piezo actuator is described figure 2. The voltage imposed to the piezo is proportional to the displacement $\mathbf{A}$. The total motion of the cantilever tip in the laboratory referential is $\mathbf{q}+\mathbf{A}$ where, $\mathbf{q}$ is the motion of the cantilever end in the base referential. The signal measured in AFM is proportional to $\mathbf{q}$. The equation of motion of the tip in the lab referential $\mathbf{q}+\mathbf{A}$ in water far from any surface is then:

$$m_0\frac{\partial^2\mathbf{q}+\mathbf{A}}{\partial t^2}+\beta_0\frac{\partial\mathbf{q}+\mathbf{A}}{\partial t}+k_0\mathbf{q}=0, \tag{1}$$

where the subscript "0" is for measurement far from any surfaces. m_0, β_0 and k_0 are respectively an effective mass, effective dissipation and effective stiffness of a cantilever mode in liquid. All these three parameters can be measured by fitting the thermal noise resonance curve, knowing the calibration factor measured in nm/V in contact mode. Here k_0 is not the stiffness of the cantilever but the stiffness of the vibration mode in liquid. It is well known that the cantilever immersed in a liquid can also be excited through the fluid in vibration [10]. This effect called "fluid- borne" excitation is studied in supplementary material. It is shown that one can neglect this effect in our experiments. As we are working in the dynamic mode at a frequency ω, one rewrites the equation with $\mathbf{q}=\mathbf{q}_0e^{j\omega t+\phi(\omega)}$ and $\mathbf{A}=\mathbf{A_{ex0}}e^{j\omega t}$:

$$(-\frac{\omega^2}{\omega_0^2}+\frac{j\omega}{\omega_0Q_0}+1)q_0e^{j\phi(\omega)}=(\frac{\omega^2}{\omega_0^2}-\frac{j\omega}{\omega_0Q_0})A_{ex0}, \tag{2}$$

where $\omega_0=\sqrt{k_0/m_0}$ and $Q_0=\frac{k_0}{\beta_0\omega_0}$. In presence of an interaction force, $\mathbf{A}=\mathbf{A_{ex}}e^{j\omega t}$. Two additional terms appear in equation (1), one in-phase $-k_{int}(qe^{j\phi(\omega)}+A_{ex})$, and one out-of-phase $-j\omega\beta_{int}(qe^{j\phi(\omega)}+A_{ex})$ with the tip motion. We assume that over one oscillation, k_{int} and β_{int} remain constant, i.e. that the oscillation amplitude is small compared to the range of interaction.This decomposition is only valid for a force for which the term in phase is proportional to the displacement and the term in out-of-phase is proportional to the velocity. Then, the equation of motion becomes:

$$\begin{aligned}(-\frac{\omega^2}{\omega_0^2}+\frac{j\omega}{\omega_0Q_0}+1)qe^{j\phi(\omega)}&=(\frac{\omega^2}{\omega_0^2}-\frac{j\omega}{\omega_0Q_0})A_{ex}\\&-\frac{k_{int}}{k_0}(qe^{j\phi(\omega)}+A_{ex})-\frac{j\omega\beta_{int}}{k_0}(qe^{j\phi(\omega)}+A_{ex}).\end{aligned} \tag{3}$$

In FM-AFM mode, the amplitude of the oscillation is kept constant so $q=q_0$ and the phase is fixed to a value that is fixed to $-\pi/2$. Let's define the corresponding frequency $\omega^0_{\pi/2}$ so that $\phi_0(\omega^0_{\pi/2})=-\pi/2$. By inserting this in equation (2), we obtain a system of two equations (real and imaginary parts) with two unknowns $\omega^0_{\pi/2}$ and q_0. After simplifying at first order in $1/Q_0$ and in frequency variation, one gets:

$$\omega^0_{\pi/2}=\omega_0(1-1/2Q_0^2), \tag{4}$$

$$q_0=A_{ex0}Q_0(1-1/2Q_0^2). \tag{5}$$

In liquid FM-AFM, we measure the frequency ω at the phase $-\pi/2$ and compare it to the reference value $\omega^0_{\pi/2}$ in

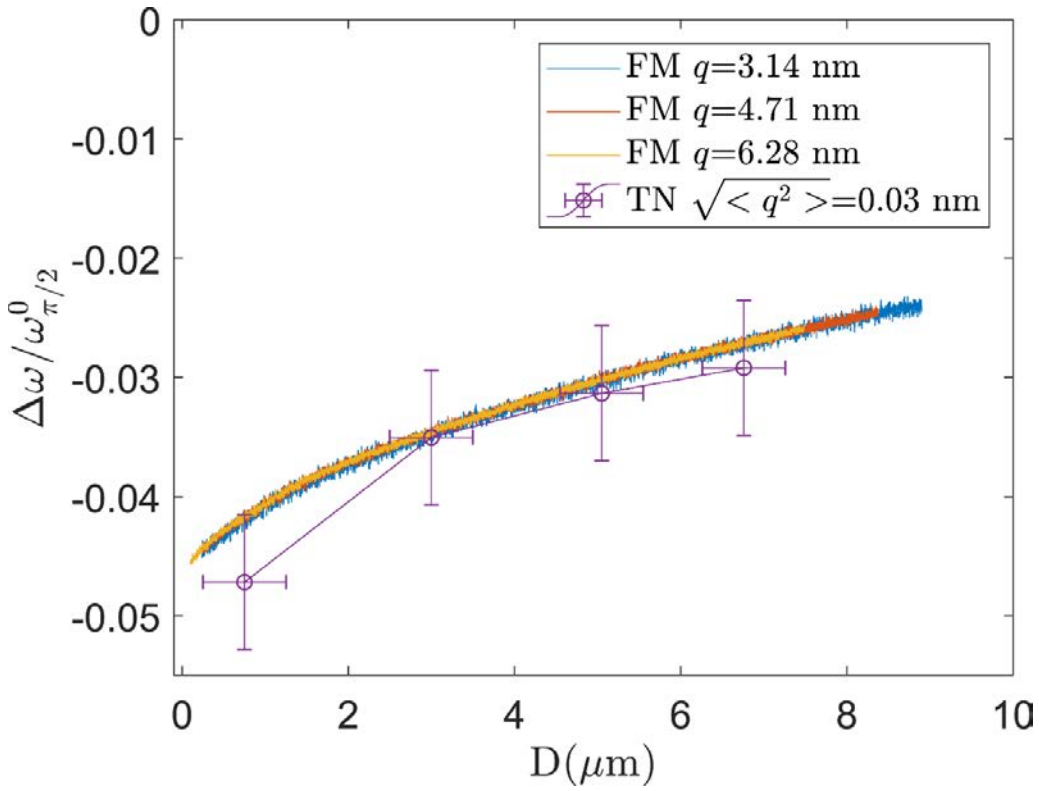

Figure 1. Resonance frequency shift of the 3rd mode of a cantilever with an 8 μ m bead versus the distance D from a glass surface in pure water. Lines: measurements for three excitation amplitudes q; symbols: resonance frequency shift in the same configuration measured by fitting the thermal noise resonance peak.

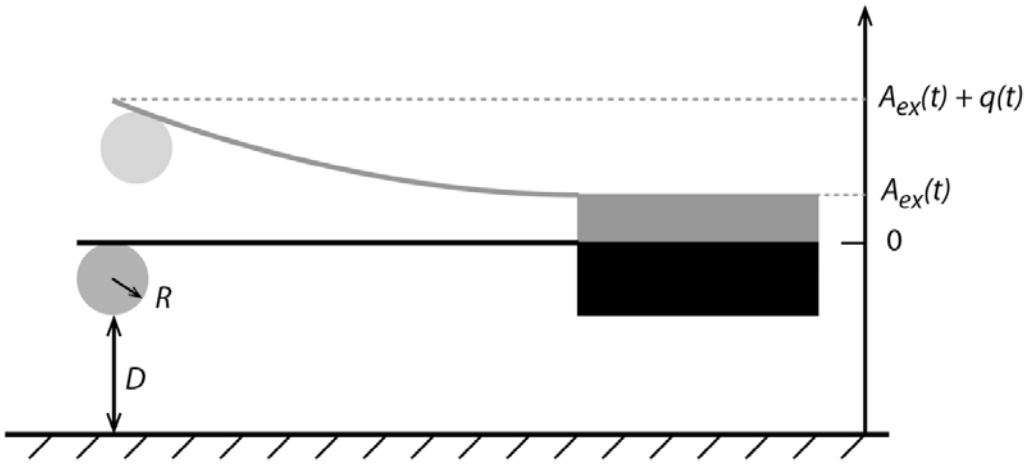

Figure 2. Sketch of the experiment. The cantilever functionalized with a bead of radius R is oscillated at a mean distance D from a solid surface. The position of the base of the cantilever is noted $A_{ex}(t)$ and its extremity $A_{ex}(t)+q(t)$ where $q(t)$ is the cantilever deflection.

absence of interaction force. We point out that $\omega^0_{\pi/2}$ differs from the natural frequency ω_0 and the resonance frequency given by $\omega_0\sqrt{1-1/2Q_0^2}$. Then, one can insert equation (5) in (3) and it gives:

$$\frac{k_{int}}{k_0} = \left(\frac{\omega}{\omega^0}\right)^2 - 1 + \frac{1}{1+Q_0^2\left(\frac{A_{ex0}}{A_{ex}}\right)^2(1-1/2Q_0^2)} \quad (6)$$

and

$$\frac{\beta_{int}}{\beta_0} = -1 + \frac{\omega_0 Q_0}{\omega}\frac{\frac{A_{ex}}{A_{ex0}}Q_0(1-1/2Q_0^2)}{\left(\frac{A_{ex}}{A_{ex0}}\right)^2 + Q_0^2(1-1/2Q_0^2)^2}. \quad (7)$$

The previous relationships can be approximated by considering that $Q_0 > A_{ex}/A_{ex0}$ in order to evidence the additional

terms in liquids compared to the relationships air:

$$\frac{k_{int}}{k_0} \approx 2\frac{\Delta\omega}{\omega^0_{\pi/2}} + \frac{1}{Q_0^2}\left(\left(\frac{A_{ex}}{A_{ex0}}\right)^2 - 1\right) \quad (8)$$

and

$$\frac{\beta_{int}}{\beta_0} \approx \frac{A_{ex}}{A_{ex0}} - 1 - \frac{A_{ex}}{A_{ex0}}\frac{\Delta\omega}{\omega^0_{\pi/2}}, \quad (9)$$

where $\Delta\omega = \omega - \omega^0_{\pi/2}$. Equations (8) and (9) clearly show that k_{int} and β_{int} both depend on the frequency shift and on the excitation amplitude, contrary to experiments in air where elastic and damping forces are separated. For typical values of $Q_0 \simeq 5$, with an amplitude ratio $A_{ex}/A_{ex0} \leq 2$, and of relative frequency shift around 1%, the second term in the right hand side of k_{int} equation is predominant. On the other hand, the third term in the right hand side β_{int} equation is small and the dissipation is barely changed compared to air. The coupling between equations (8) and (9) is based on the assumption that the in-phase and out-of-phase parts of the interaction force are proportional to the displacement and the velocity, respectively. Note that the approximate equation (9) is identical to that obtained by Suzuki *et al* [17]. The case of arbitrarily large oscillation amplitudes was treated in the literature [18] but provides expressions which are more difficult to use in practice.

3. Long range FM-AFM experiments

A specific experiment is developed in order to characterize the effects of hydrodynamic forces at short and long distance. A JPK Nanowizard 3 AFM is employed in FM-AFM mode and thermal noise mode to measure the frequency shift and the dissipation versus the distance to a glass surface D. For thermal noise measurements, the signal from the cantilever deflection is recorded at a high sampling rate (400 kHz) during 2 s at fixed sample-tip separation. For FM experiments, the PLL device of the signal access module Vortis JPK operates two feedbacks, one on the excitation frequency to maintain the phase constant and one on the excitation amplitude A_{ex} to maintain the tip oscillation constant. The resulting angular frequency shift $\Delta\omega$ and A_{ex} are monitored in function of D.

The cantilever used is NanoW Arrow TL. Since the first resonance frequency is too low to be efficiently excited by the piezo shaker available, we work with higher translational modes. This permits to have a higher Q factor as well, $Q_0 \simeq 5$. The cantilever stiffness k_0 is characterized for a given mode by thermal noise using the deflection sensitivity derived from contact mode experiments on a glass wafer substrate [18].

The probe-substrate distance D is calculated by the difference between the piezo elevation and the cantilever deflection although in most of the range of our measurements, the cantilever deflection is close to zero.

Cantilevers are functionalized with beads of radius $R = 8.3\mu$m (Duke Standards, dry, Borosilicate) and $R = 20.6\mu$m (Dynoseeds TS, dry, Polystyrene). There are glued at the end of the cantilever thanks to NOA 68 and insulated under UV lamp for 10 min. All AFM experiments are realized in deionized water. When performing experiments above glass, the cell is carefully rinsed with isopropanol, ethanol then water.

We perform two series of experiments against a glass surface in water at an approaching speed of 1μm s^{-1}: one at ''short'' distance within the 15 μ m range piezo displacement in order to study the influence of the oscillation amplitude; one at large distance up to 160 μ m, where the cantilever is moved by alternatively by the step motor and the piezo transducer. The reference values of A_{ex0} and $\omega_0^{\pi/2}$ are measured at distance larger than 200μm for which no variation of the frequency is observed.

4. Results and discussion

Figure 1 shows the shift in frequency for different tip oscillations q. We observe a decreasing frequency when approaching the wall as previously observed [17]. This is equivalent in AM-AFM mode of a phase decrease [11]. We observe a perfect match for different oscillation amplitudes. Even with thermal noise excitation, the amplitude of excitation of which is very low, we measure similar variations in resonance frequency. Thus, decreasing the oscillation amplitude will not decrease the frequency shift. These results suggest that hydrodynamic forces are responsible for this behavior [13]. In order to verify this assumption, we performed AFM experiments in liquid at large distance, far above the characteristic lengths of molecular and electrostatic interactions. We performed experiments up to 200 μm for the biggest bead we were able to glue that provide a nice resonance peak with a radius $R = 20.6\mu$m and a width $b = 100\mu$m in order to maximize the hydrodynamic forces.

Thanks to equation (6) and (7), we plot k_{int}/k_0 and β_{int}/β_0 respectively in figure 3 and 4. Interestingly, the hydrodynamic forces induce a variation of the in-phase parameter over a range of distance of order of 100 μm. In comparison, the variation of the out-of-phase component is confined within 10 μm and is close to zero beyond. The decrease of k_{int} was also observed with $R = 8.3\mu$m bead as shown at short distance in figure 1. Note that dynamic AFM in non-elastic (Newtonian) liquid generates at large distance hydrodynamic forces for which the in-phase component can be on a same order of magnitude that the one in out-of-phase. Whereas the damping increase of an oscillating sphere near a wall has already been well characterized both experimentally and numerically in the lubrication approximation $R >> D$, the decrease of k_{int} that accounts for the added-mass increase as D decreases [14] has attracted less attention.

Recently, the hydrodynamic force exerted on an oscillating bead near a wall was analytically calculated for various limit cases [19]. Three main parameters are R the bead radius, $H = R + D$ the distance between the bead center and the wall, and $\delta = \sqrt{\nu/\omega}$, the size of the boundary layer. In the experimental conditions of figure 3 and 4, we obtain $\delta \approx 4\mu$m.

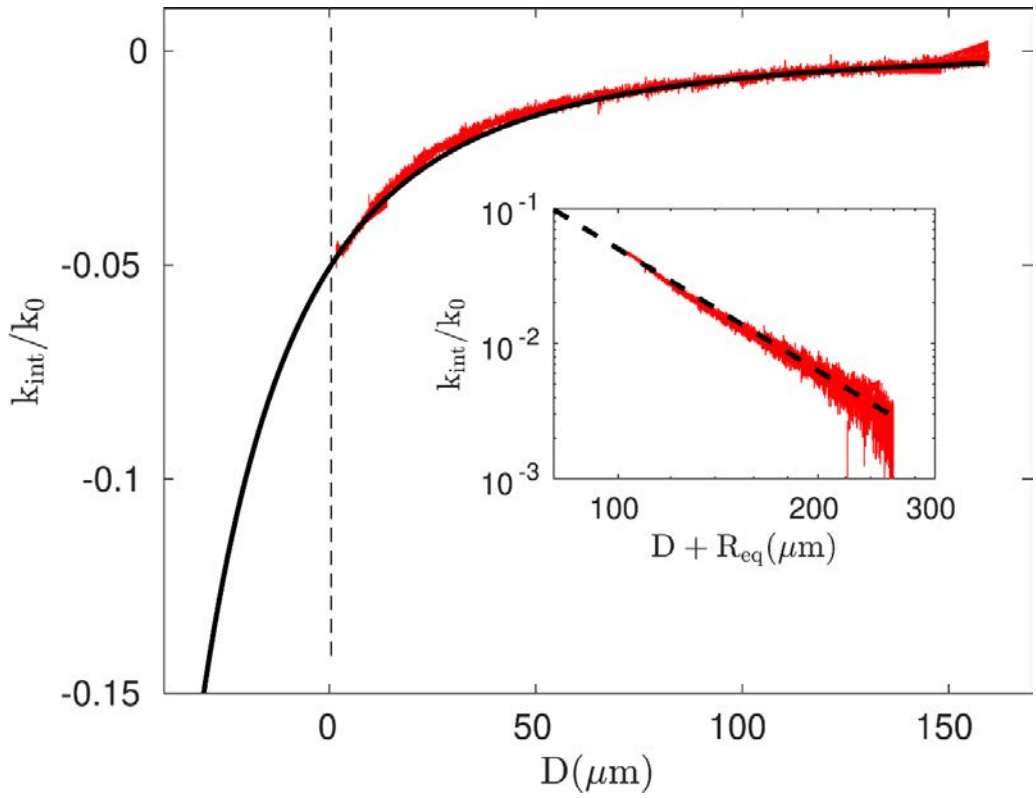

Figure 3. Evolution of k_{int}/k_0 vs the distance D measured in long range FM-AFM experiments (red symbols). Comparison with the model of an oscillating bead in a liquid close to a wall (black line). Inset: verification of the power law in -3 in agreement with equation (11).

For $H>>R$ and $H>>\delta$ corresponding to our experiments for which the flow is unsteady, the normalized perpendicular force exerted by the fluid on the bead F_N is given by:

$$F_N = -\frac{3\pi R^3}{4\,\mathrm{H}^3}\left(5+3\sqrt{2/\Omega}+\sqrt{2\Omega}\right)V_\perp - j\frac{3\pi R^3}{4\,\mathrm{H}^3}\left(3/\Omega+3\sqrt{2/\Omega}-\Omega/3-\sqrt{2\Omega}\right)V_\perp \quad (10)$$

where $\Omega = R^2\omega/\nu$ is the Reynolds number for a sphere and $V_\perp$ is the dimensionless perpendicular velocity of the bead. $V_\perp = 1$ if the movement is purely perpendicular to the wall. In this equation, the force is normalized by $\rho\nu RV$ where V is the bead velocity. Rewriting this force in term of k_{int} and β_{int}, we obtain:

$$k_{int} = \rho\nu R\omega\frac{3\pi R^3}{4\,\mathrm{H}^3}(3/\Omega+3\sqrt{2/\Omega}-\sqrt{2\Omega}-\Omega/3), \quad (11)$$

and

$$\beta_{int} = \rho\nu R\frac{3\pi R^3}{4\,\mathrm{H}^3}(5+3\sqrt{2/\Omega}+\sqrt{2\Omega}). \quad (12)$$

This model is compared with the experimental results in figure 3 and 4. The stiffness and the resonant frequency characteristic of the second mode that is used in these FM-AFM experiments are measured by thermal noise with optical lever correction: $k_0 = 4.8$ N m^{-1} and $\omega_0 = 77.9\times10^3$ rad s^{-1}. Due to the respective dimensions of the probe ($R = 20.6$ μm) and of the cantilever (100×500 μm^2), the hydrodynamic forces arise mainly from the cantilever vibration at large distance. In order to compare the results with the model, the cantilever is assimilated to a sphere with an equivalent radius R_{eq} and the origin of its displacement is defined by $D=-2$ R. Indeed, at $D=0$, the cantilever is at a distance of 2 R due to the presence of bead probe. The experimental results are fitted by the model with R_{eq} as the only free parameter. We found a very good agreement between model and experiments for $R_{eq} = 59$ μm for the curves of k_{int}/k_0. We check that $2R_{eq}$ is comprised between the length and the width of the cantilever. The inset of figure 3 shows that the experimental data follow the power-law in $(D+R_{eq})^{-3}$ in the whole range of the experimental distance as predicted by equation (11). On the other hand, the bead model points out clearly that β_{int}/β_0 is small, within the experimental noise, in agreement with the experiments at large distance. However, it cannot predict the divergence of the dissipation when the bead attached at the extremity of the cantilever approaches the substrate. In this case, the dissipation is simply given by the Reynolds formulae $\beta_{int} = 6\pi\eta R^2/D$ calculated in lubrication assumptions (steady flow) for the probe of radius R and $D\lesssim\delta$. The inset of figure 4 shows the very good agreement between the Reynolds model and the experimental data, in accordance with the literature [11, 15, 16]. The situation is different for k_{int} since the Reynolds force associated with the probe has no in-phase component. As seen in figure 3 no deviation from the oscillating bead model for the cantilever is observed at short distance.

Hence, the hydrodynamic forces arise from the oscillating cantilever and from the bead probe at its extremity. The

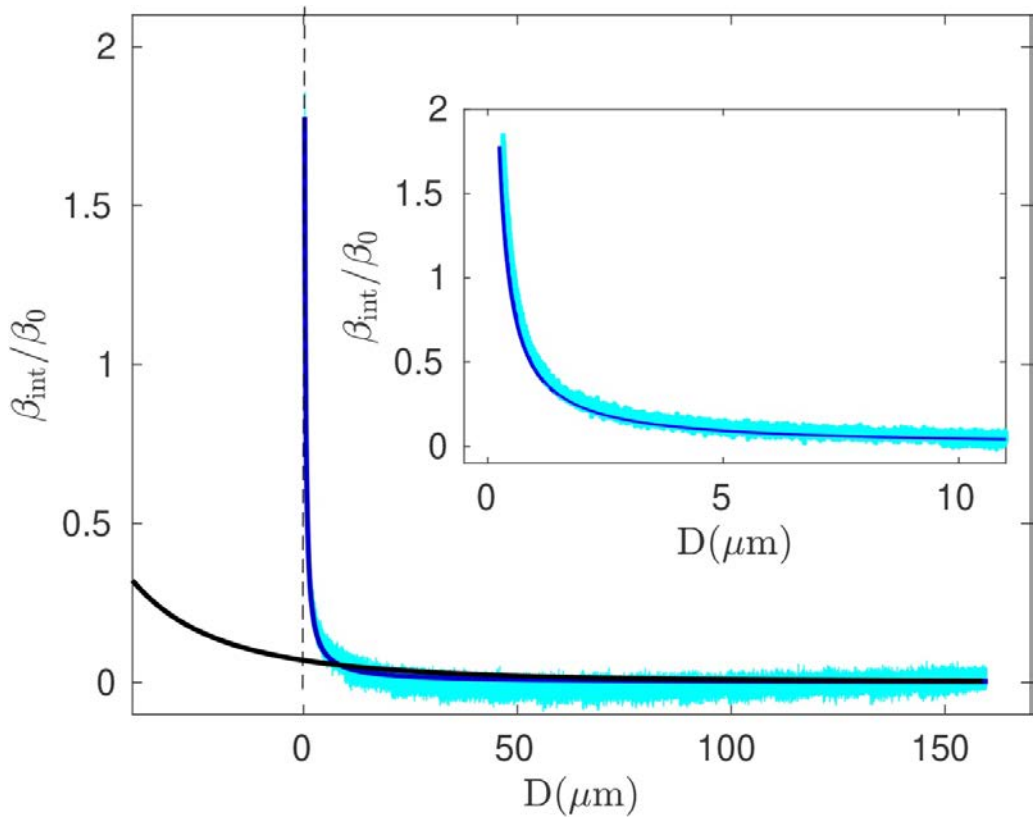

Figure 4. Evolution of β_{int}/β_0 vs the distance D measured in long range FM-AFM experiments (blue symbols). Comparison with the model of an oscillating bead in a liquid close to a wall (equation (12), black line) and with the Reynolds model (blue line). Inset: comparison of experimental data of β_{int}/β_0 and Reynolds model at short distance.

force on cantilever is effective at very large distance up to 200 μm and is mainly observed on the in-phase k_{int}/k_0 component. The Reynolds force on the bead probe occurs at short distance ($D \lesssim \delta$) and is only observed on the out-of-phase β_{int}/β_0 component. In this range of distance, the dissipation due to the force on the cantilever is negligible. We can compare the experimental data at $D = 10\mu$m to those obtained by numerical simulations. We measure an in-phase and out-of-phase components of the hydrodynamic load of 0.8 nN and 0.6 nN, respectively. Estimation using published numerical simulations [13] leads to hydrodynamic forces of about 1 nN, both for the conservative and dissipative components, in agreement with the experiments and the analytical model. Equations (11) and (12) can therefore be used to deduce the equivalent radius of the cantilever by fitting data at large distance. The long range hydrodynamic interaction due to the cantilever can then be subtracted from the total signal to infer molecular interactions between the probe and the surface at short distance.

5. Conclusion

FM-AFM experiments in liquid require to take into account the hydrodynamic forces that influence measurements of the frequency shift and of the dissipation. Theoretically, we have shown that the frequency shift and the excitation amplitude are dependent on the in-phase component k_{int} and out-of-phase component β_{int} of the interaction forces including hydrodynamic forces. We have established the relationships which can be used to extract k_{int} and β_{int} from the experimental raw data. Specific FM-AFM experiments have been developed in conditions where the cantilever and the bead probe are submitted to hydrodynamic forces. The results were analyzed in the frame of a hydrodynamic model of one sphere oscillating near a wall. The experiments point out that the evolution of k_{int} with the distance arise from the unsteady hydrodynamic forces on the cantilever over a large range of displacement. On the other hand, the evolution of β_{int} is observed at short distance and is due to the Reynolds force on the bead probe. Finally, we investigate the effects of the fluid-borne interactions (in the supplementary material) and showed that these forces do not influence the measurements in FM-AFM. This work allows us to analyze easily FM-AFM experiments in liquid in order to extract the interaction force between tip and sample. Indeed, it shows that the dissipated force between a probe and a surface can be analyzed using the Reynolds model with confidence at short distance. Moreover, the measurement of molecular interaction force between the probe and the surface based on k_{int} determination requires to subtract the effects of hydrodynamic forces on the cantilever. This can be achieved using equation (11). This study may therefore broaden the use of FM-AFM in liquid.

6. Supplementary material

See supplementary material (link) to have the details calculations for FM-AFM formulae including fluid-borne forces and their effects in data of the present paper.

Acknowledgment

The authors thank the Institut Carnot Isifor which funded the RIC project and allowed us to realize this study.

ORCID iD

Philippe Tordjeman https://orcid.org/0000-0002-6470-9081

References

[1] Israelachvili J 2011 *Intermolecular and Surface Forces* (Amsterdam: Elsevier)

[2] Garcia R 2010 *Amplitude Modulation Atomic Force Microscopy* (Weinheim, Germany: Wiley-VCH Verlag & Co.)

[3] Morita S, Giessibl F J, Meyer E and Wiesendanger R 2019 *Noncontact Atomic Force Microscopy* (Switzerland: Springer)

[4] Dufrene Y F, Ando T, Garcia R, Alsteens D, Martinez-Martin D, Engel A, Gerber C and Mueller D J 2017 Imaging modes of atomic force microscopy for application in molecular and cell biology *Nature Nanotech.* **12** 295–307

[5] Fukuma T, Ueda Y, Yoshioka S and Asakawa H 2010 Atomic-scale distribution of water molecules at the mica-water interface visualized by three-dimensional scanning force microscopy *Phys. Rev. Lett.* **104** 016101

[6] van Lin S R, Grotz K K, Siretanu I, Schwierz N and Mugele F 2019 Ion-specific and ph-dependent hydration of mica–electrolyte interfaces *Langmuir* **35** 5737–45 PMID: 30974056

[7] Ando T, Uchihashi T and Fukuma T 2008 High-speed atomic force microscopy for nano-visualization of dynamic biomolecular processes *Prog. Surf. Sci.* **83** 337–437

[8] Baró A M and Reifenberger R G 2012 *Atomic Force Microscopy in Liquid: Biological Applications* (Germany: Wiley-VCH Verlag & Co., Weinheim)

[9] Putman C A J, Van der Werf K O, De Grooth B G, Van Hulst N F and Greve J 1994 Tapping mode atomic force microscopy in liquid *Appl. Phys. Lett.* **64** 2454–6

[10] Kiracofe D and Raman A 2011 Quantitative force and dissipation measurements in liquids using piezo-excited atomic force microscopy: a unifying theory *Nanotechnology* **22** 485502

[11] Maali A and Boisgard R 2013 Precise damping and stiffness extraction in acoustic driven cantilever in liquid *J. Appl. Phys.* **114** 144302

[12] Sader J E 1998 Frequency response of cantilever beams immersed in viscous fluids with applications to the atomic force microscope *J. Appl. Phys.* **84** 64–76

[13] Green C P and Sader J E 2005 Small amplitude oscillations of a thin beam immersed in a viscous fluid near a solid surface *Phys. Fluids* **17** 073102

[14] Basak S, Raman A and Garimella S V 2006 Hydrodynamic loading of microcantilevers vibrating in viscous fluids *J. Appl. Phys.* **99** 114906

[15] Maali A, Cohen-Bouhacina T and Kellay H 2008 Measurement of the slip length of water flow on graphite surface *Appl. Phys. Lett.* **92** 053101

[16] Comtet J, Nigues A, Kaiser V, Coasne B, Bocquet L and Siria A 2017 Nanoscale capillary freezing of ionic liquids confined between metallic interfaces and the role of electronic screening *Nature Mat.* **16** 634–9

[17] Suzuki K, Kobayashi K, Labuda A, Matsushige K and Yamada H 2014 Accurate formula for dissipative interaction in frequency modulation atomic force microscopy *Appl. Phys. Lett.* **105** 233105

[18] Sader J E, Uchihashi T, Higgins M J, Farrell A, Nakayama Y and Jarvis S P 2005 Quantitative force measurements using frequency modulation atomic force microscopy?theoretical foundations *Nanotechnology* **16** S94–S101

[19] Fouxon I and Leshansky A 2018 Fundamental solution of unsteady stokes equations and force on an oscillating sphere near a wall *Phys. Rev.* E **98** 063108